Coordination of an amino alcoholic Schiff base ligand toward zinc(II) ion: Spectral, structural, theoretical and docking studies

Javad Esmaeilzadeh[a], Zahra Mardani[a,]*, Keyvan Moeini[b], Cameron Carpenter-Warren[c], Alexandra M. Z. Slawin[c] and J. Derek Woollins[c]

[a] Inorganic Chemistry Department, Faculty of Chemistry, Urmia University, 57561-51818, Urmia, I. R. Iran

[b] Department of Chemistry, Payame Noor University, 19395-4697 Tehran, I.R. of Iran

[c] EaStCHEM School of Chemistry, University of St Andrews, St Andrews Fife UK, KY16 9ST

*Corresponding author:
E-mail: z.mardani@urmia.ac.ir
Fax: +98 4432752746

Abstract: A new zinc(II) complex of 2-(((2-((2-hydroxyethyl)amino)ethyl)imino)methyl)phenol (L), $[Zn(L^z)Br_2]$ (**1**), was prepared and identified by elemental analysis, FT-IR and ^{1}H NMR spectroscopy and single-crystal X-ray diffraction. X-ray structure analysis of **1** revealed a tetrahedrally coordinated zinc(II) complex containing NO-donor amino alcoholic Schiff base ligand and two bromo ligands. After complexation, the ligand (L) converts to its zwitterionc form (L^z) of phenol→phenolate; amine→ammonium. In this structure, the hydrogen bonds between amine and alcohol units form different types of hydrogen bond motifs including, $R_2^1(7)$, $R_2^2(7)$, $R_2^2(10)$, $R_4^4(24)$, $R_4^4(30)$, $R_6^6(38)$ and $R_6^6(44)$. In addition to the hydrogen bonds in this crystal network, there are π–π stacking interactions between phenyl ring with imine group. The ability of the ligand and its isostructural complexes with $ZnCl_2$, $ZnBr_2$ and ZnI_2 to interact with ten selected biomacromolecules (BRAF kinase, CatB, DNA gyrase,

HDAC7, rHA, RNR, TrxR, TS, Top II and B-DNA) was investigated by docking studies. The results showed that in some cases, the studied compound can interact with proteins and DNA better than doxorubicin. The charge distribution pattern of the ligand and its complex **1** was studied by NBO analysis.

Keywords: amino alcohol, Schiff base, zinc, docking study, DFT, protein

Introduction

The amino alcohol unit is widely described as scaffold of many biologically active compounds, with a great variety of pharmacological effects. Many *β*-amino alcohols exhibit a broad spectrum of biological activities such as antibacterial and tuberculostatic agents [1]. The *γ*-secretase inhibitory activity and Notch-sparing effects were reported for some *γ*-amino alcohols [2]. Some of them are used as active pharmaceutical ingredients (API's) such as *α*- and/or *β*-adrenergic agonists [3, 4], HIV protease inhibitors [5] and anti-hypertensive activity by blocking the *α*- and/or *β*-adrenergic receptors [6, 7]. The interactions of this class of compounds toward DNA and proteins were established by docking studies [8-11].

Schiff bases and their complexes have played an important role in the development of coordination chemistry, biological and material science. Schiff base ligands and their complexes show interesting pharmacological effects such as antimicrobial [12], antitumor [13, 14], antibacterial [15], antifungal [15], antioxidative [16], and urease inhibitory [17, 18] activities. The cleavage of plasmid DNA by Schiff base complexes has also been reported [19, 20]. Some studies revealed that the anti-cancer, anti-bacterial and anti-viral activities of Schiff base ligands tend to increase in binding to metal centers [21, 22].

Based on the biologically active properties of the Schiff base and amino alcoholic units, we decided to synthesis a ligand and complexes containing these moieties. As a part

of our systematic studies, in this contribution, we present the synthesis, crystal, molecular and the spectroscopic characterization of the zinc(II) complex, [Zn(L^z)Br_2] (**1**), with 2-(((2-((2-hydroxyethyl)amino)ethyl)imino)methyl)phenol ligand (L, Fig. 1) along with the theoretical studies. The amino alcoholic Schiff base ligand of L^z is in its zwitterionic form and the hydrogen atom of the phenol group was moved on the amine group.

Please insert Figure 1 here.

In addition to the expected biological properties of amino alcoholic Schiff base ligand, L, binding it to Zn(II) ion makes this complex a good choice for a biologically active compound [8, 23-26]. For study of the biological activities of the ligand and its zinc(II) complex, docking calculations were performed to investigate the possibility of an interaction between these compounds with ten biomacromolecule targets [8, 26-30], including: BRAF kinase, Cathepsin B (CatB), DNA gyrase, Histone deacetylase (HDAC7), recombinant Human albumin (rHA), Ribonucleotide reductases (RNR), Thioredoxin reductase (TrxR), Thymidylate synthase (TS), Topoisomerase II (Top II) and B-DNA. These proteins were selected either due to their reported roles in cancer growth or as transport agents that affect drug pharmacokinetic properties (e.g., rHA). The DNA gyrase was included to study the possibility of anticancer properties and their activity as antimalarial agents [8].

Results and Discussion

The ligand L was prepared by the condensation of 2-hydroxybenzaldehyde and 2-((2-aminoethyl)amino)ethan-1-ol with 1:1 molar ratio. Reaction of zinc(II) bromide with L provided complex **1**. During the complexation reaction the ligand converts to its zwitter ionic form (L^z). The complex is air-stable and soluble in DMSO.

Spectroscopic characterization

Study of the IR spectrum of **1** revealed that there are different types of moieties in this structure for example, *v* (C−H) aromatic, *v* (O−H) alcoholic and *v* (N−H) amine at above 3000 cm^{-1}, *v* (C−H) aliphatic at near 3000 cm^{-1} and *v* (C=N) imine at near 1550 cm^{-1}. A peak corresponding to the amine group is shifted 59 cm^{-1} to lower frequencies respect to the free ligand [31]. This shifts have been reported previously for alkylammonium ions [32, 33] and confirming the formation of zwitterionic form of ligand. Another evidence for protonation of the amine group is appearing a peak at 1630 cm^{-1} due to the bending vibration of $R_2NH_2^+$. The imine group of the ligand is shifted 59 cm^{-1} to lower frequencies after coordination to zinc(II) ion, confirming the coordination through the nitrogen atom of this unit. Study of the ^{1}H NMR spectrum of **1** revealed that the phenolic proton of the ligand is missed and a new peck at the aliphatic region is appeared which is the another reason for formation of the zwitterionic form of the ligand after complexation.

Crystal structure of [Zn(L^z)Br_2] (1)

X-ray analysis of **1** revealed a rare zwitterionic complex of zinc(II) ion (Fig. 2). In the crystal structure of **1**, the zinc(II) ion is tetra-coordinated by one imine nitrogen and one phenolate oxygen atom of the ligand along with two bromo ligands. In the tetra-coordinated zinc complexes, donor atoms commonly arrange in a tetrahedral and rare in a square planar configuration. To determine the coordination geometry of the zinc(II) ion in this complex, the angular structural parameter τ_{sq} was calculated using the formula introduced by Hakimi *et al.* [34]. The index of tetragonality (τ_{sq}) is defined by (θ_{max}–θ_{min})/90, where θ_{max} and θ_{min} are the maximum and minimum bond angles, respectively. For an ideal square plane, θ_{max} = 180º and θ_{min} = 90º and τ_{sq} = 1; however, an ideal tetrahedron will have θ_{max} = 109.28º, θ_{min} = 109.28º and therefore τ_{sq} = 0. The calculated τ_{sq} value for this complex is 0.19, indicating a propensity to a tetrahedral geometry (Fig. 3) and in agree with the literature. Comparing the bond length value for Zn–O, Zn–N and Zn–Br (1.96(1), 2.01(2) and 2.376 Å, respectively)

in **1** with Cambridge structural database (CSD) [35] average (1.956, 2.013 and 2.368 Å, respectively) revealed that all bond lengths are comparable (for precise result, all tetra coordinated zinc(II) complexes containing two non-bridging bromo ligands and an NO-donor ligand with six-membered chelate ring were selected). In this complex, the bond angle of Br–Zn–Br is 15.98º bigger than the N–Zn–O. Similar result was observed among the CSD analogues (19.43º).

Please insert Figure 2 here.

Please insert Figure 3 here.

In the molecular structure of **1**, the amino alcoholic ligand acts as a bidentate and forms a planar six-membered chelate ring (maximum deviation from the mean plane through the chelate ring for O004 atom, 0.047 Å). Although the phenolic group of the ligand was deprotonated during the complexation reaction, but owing to proton transfer from phenol to amine group, this ligand remains neutral and thus the ligand is coordinated to zinc(II) ion in its zwitterionic form. Study of the all complexes of L among the CSD revealed that this ligand has four coordination modes (Fig. 4). In all coordination modes the phenolic group is deprotonated and in rare condition after deprotonation of the phenol group a zwitterion isomer (3%) is formed. Based on these data we can consider this ligand as acidic HL. Also this ligand can bridge between two metals through the phenolate unit (9%). Among the observed bidentate, tridentate and tetradentate coordination modes of this ligand the tridentate ($O^{phenol}N^{imine}N^{amine}$) (Fig. 4) mode is common (63%).

Please insert Figure 4 here.

In the crystal network of **1**, there are C–H···Br, N–H···O, O–H···N and O–H···O hydrogen bonds. Among them the N–H···O and O–H···O form different types of hydrogen

bond motifs including, $R_2^2(10)$ (two acceptors, two donors with degree of 10) [36, 37], $R_2^1(7)$, $R_2^2(7)$, $R_4^4(24)$, $R_4^4(30)$, $R_6^6(38)$ and $R_6^6(44)$ (Fig. 3). For formation of these motifs the amine and alcohol units of the ligand have the main role.

In addition to these hydrogen bonds, the crystal packing features π–π stacking interactions [28, 38] between phenyl ring with imine group. The centroid-centroid distance between the π systems of two connected units is 3.606 Å and these units are not exactly on top of each other.

Theoretical studies

To study the charge distribution before and after complexation, an NBO analysis was done on the ligand and complex **2** (Table 1). For precise study we used the geometrical parameters of the solid state form for ligand and its complex **1**. The results reveal that the calculated charge on the zinc atom (+0.94) is 1.06 lower than the formal charge (+2) owing to the electron donation of ligand during the complexation reaction. Based on the calculated average charge values of structures, the charge on the bromide ion is 0.39 positive than its formula charge (–1), confirming that this ligand has important role in electron donation toward zin(II) ion and decreasing the charge on it. Also the charge of the carbon atoms and oxygen atom of the alcoholic group is slightly positive than respect to the free ligand and have same role as bromo ligands [27, 38-40]. The average charge of bonded nitrogen and oxygen atoms is negative than respect to their free ligands. This observation reveals that these atoms owing to their high electronegativity withdraw electron density from zinc(II) ion [27, 38-40]. The charge on the nitrogen atom of the amine unit is 0.17 positive than the free ligand due to the proton transfer of phenol to the amine unit and formation of ammonium unit.

Please insert Table 1 here.

Docking studies

For predicting the biological activity of ligand and its complex **1**, interactions of these compounds with ten macromolecular receptors were studied using Gold [41] docking software. The Gold docking results are reported in terms of the values of fitness which means that the higher fitness the better the docking interaction of the compounds [8, 26-30]. For evaluation of the calculated fitness values, these scores were compared with those of the famous anti-cancer drug, doxorubicin (a cancer medication that interferes with the growth and spread of cancer cells in the body [29, 42]).

It is interesting that comparing the docking results of **1** with isostructural complexes of chloride, iodide and fluoride analogues. Study of the CSD revealed that the structure of chloride (isostructural with **1**) analogue has been reported previously [43] and also structure of other analogues could be guessed using the CSD. Searching the CSD for complexes containing unit presented at Fig. 5 (X refers to the halogen atoms) revealed that there are 18 examples for such complexes. Among them 16 examples [16, 43-56] are containing an amine moiety in structure of ligand and are close to our new record. In all 16 complexes the hydrogen atom of the phenol unit was transferred on the amine group and all ligands are in their zwitter ionic form (similar with **1**). This study revealed that the zwitterionic structure is commonly form in reaction between zinc(II) halides with ligand containing phenol, imine and amine groups. Thus the structure of the iodide and fluoride analogues could be determined by DFT calculation.

Please insert Figure 5 here.

Among the 18 examples, there is no hit containing fluoride ion. It seems that this ion forms different structure than the other halogen ions. Study of the CSD revealed that there is

no record for $ZnNOF_2$ environment. Thus the optimization of the fluoride analogue was omitted from the DFT calculation owing to the non-possibility of this structure.

The general features from the Gold docking prediction (Table 2) show that all studied compounds can be considered as biologically active compound [8, 27, 28, 30]. The best predicted protein target for ligand and complexes **1**–**3** is HDAC7. Based on the calculated fitness values, in each case, the binding ability of one, two or three complexes is higher than that of the free ligand [57]. Docking calculations revealed that all studied compounds have higher fitness scores compared to doxorubicin in binding toward CatB and HDAC7. Data shown in Table 2 revealed that these compounds can place in the major and minor grooves of the DNA molecule which make these compounds a good choice for DNA binding studies. Attaching ability of the new compounds into major and minor grooves of DNA molecule is higher and lower than the doxorubicin, respectively. The docking results of the interaction between the ligand and complex **1** with B-DNA (major and minor grooves) are shown in figures 6 and 7, respectively.

Please insert Figure 6 here.

Please insert Figure 7 here.

Please insert Table 2 here.

Conclusion

In this work, a new amino alcoholic Schiff base zinc(II) complex, $[Zn(L^z)Br_2]$ (**1**); L: 2-(((2-((2-hydroxyethyl)amino)ethyl)imino)methyl)phenol, was synthesized and its spectral and

structural properties were investigated. X-ray analysis of **1** revealed that during the complexation process the zwitterionic form of ligand (L^z) was formed by deprotonation of phenol unit and protonation of amine group. In this structure the L^z acts as NO-donor which is the rare coordination mode for this type of ligands among the CSD analogues. The zinc atom is tetrahedrally coordinated with $ZnNOBr_2$ environment. In this structure, the amine and alcoholic moieties play an important role in hydrogen bonding and form different types of hydrogen bond motifs including, $R_2^1(7)$, $R_2^2(7)$, $R_2^2(10)$, $R_4^4(24)$, $R_4^4(30)$, $R_6^6(38)$ and $R_6^6(44)$. The phenyl ring and imine unite participates in formation of π–π stacking interactions. Docking studies revealed that the ligand and complexes **1**–**3** can interact with ten biomacromolecules (BRAF kinase, CatB, DNA gyrase, HDAC7, rHA, RNR, TrxR, TS, Top II and B-DNA). The best predicted target for all studied compounds is HDAC7. Since the fitness values of the studied compounds in some cases (CatB, HDAC7 and B-DNA major groove) are higher than those of doxorubicin, studying anticancer activities of it could be interesting. The NBO analysis of the complex **1** along with its free ligand revealed that the carbon and alcoholic oxygen atoms along with bromide ions act as electron donor and decrease the charge of the zinc atom.

Experimental

Materials and Instrumentation

All starting chemicals and solvents (Merck, Aldrich) were used
as received without further purification. The L ligand was prepared as described in previous work [31]. The infrared spectrum (as KBr pellet) in the range 400–4000 cm^{-1} was recorded with a Shimadzu FT-IR 8400 spectrometer. The carbon, hydrogen and nitrogen contents were determined using a Thermo Finnigan Flash Elemental Analyzer 1112 EA. ^1H NMR spectra were recorded on a Bruker Avance 300 instrument operating at 300 MHz; chemical

shifts are given in parts per million, with values referenced to internal TMS. The melting point was measured with a Barnsted Electrothermal 9200 electrically heated apparatus.

Preparation of [Zn(L^z)Br$_2$] (1)

A solution of 0.42 g (2 mmol) of L in MeOH (10 mL), was added with stirring to solution of 0.45 g (2 mmol) of $ZnBr_2$ in the same solvent (25 mL). The reaction mixture was then heated to reflux for six hours. Yellow crystals suitable for X-ray diffraction were obtained by slow evaporation of the solution after several days and were collected by filtration. Yield 0.24 g, 22%. M.p. 188 °C. Anal. calcd. for $C_{11}H_{16}Br_2N_2O_2Zn$ (537.55): C, 30.48; H, 3.72; N, 6.46. Found C, 30.59; H, 3.77; N, 6.48. IR (KBr disk): 3501 (ν O−H), 3105 (ν N−H), 3015 (ν C−H)^{ar}, 2951 (ν_{as} CH_2), 2903 (ν_s CH_2), 1630 (δ_s NH_2), 1544 (ν C=N), 1464 (ν C=C), 1446 (δ_{as} CH_2), 1403 (δ_s CH_2), 1248 (ν C−O), 1064 (ν C−N) cm^{-1}. ^{1}H NMR (300 MHz, [D$_6$]DMSO): 8.4 (s, 1H, CH^{imine}), 6.5−7.3 (m, 4H, CH^{ar}), 2.1–3.7 (m, 11H, NH_2^+, CH_2, OH^{alc}) ppm.

Crystal structure determination and refinement

Diffraction data were collected at 173 K on a Rigaku FRX RA/Pilatus 200 equipped with a (Mo Kα radiation, λ = 0.71073 Å). All data were corrected for Lorentz and polarization and absorption effects. The structure was solved by using SHELXT and refined by full-matrix least-squares refinement against F^2 by using SHELXL [59].

Refs Sheldrick, G. M. (2014). Acta Cryst. (2014). A70, C1437.

SHELXT Version 2018/2

Sheldrick, G.M. (2008) SHELXL Version 2018/3, Acta Cryst. A64, 112-122.

Hydrogen atoms were included on idealized positions (riding model). Selected crystallographic data are presented in Table 3. Selected bond lengths are displayed in Table 4, hydrogen bond data in Table 5. Diagrams of the molecular structure were created using Ortep-III [60, 61] and Diamond [62].

Please insert Tables 3–5 here.

Computational details

The complex **3** was optimized with the Gaussian 09 software [63] and calculated for an isolated molecule using Density Functional Theory (DFT) [64] at the B3LYP/LanL2DZ level of theory. Also NBO analysis were calculated for an isolated molecule using DFT at the B3LYP/6-31G(d,p) and B3LYP/LanL2DZ level of theory for ligand and complex **1**, respectively. Cif file of the ligand and complex **1** was used as input file for theoretical calculations.

Docking details

The pdb files 4r5y, 3ai8, 5cdn, 3c0z, 2bx8, 1peo, 3qfa, 1njb, 4gfh and 1bna for the ten receptors, BRAF kinase, Cathepsin B (CatB), DNA gyrase, Histone deacetylase (HDAC7), recombinant Human albumin (rHA), Ribonucleotide reductases (RNR), Thioredoxin reductase (TrxR), Thymidylate synthase (TS), Topoisomerase II (Top II) and B-DNA, respectively, used in this research were obtained from the Protein Data Bank (PDB) [65]. The full version of Genetic Optimization for Ligand Docking (GOLD) 5.5 was used for the docking studies. The Hermes visualizer in the GOLD Suite was used to further prepare the compounds and the receptors for docking. The cif file of the ligand and complexes **1** and **2** were used for the docking studies. The structure of the complex **3** was optimized by DFT

calculation and then used for docking studies. The region of interest used for GOLD docking was defined as all the protein residues within 6 Å of the reference ligand "A" that accompanied the downloaded protein. For B-DNA, the region of interest was defined on DNA backbone within 10 Å of the O4, DT19 and O2, DT19 atoms for major and minor graves, respectively. All free water molecules in the structure of the proteins were deleted before docking. Default values of all other parameters were used and the compounds were submitted to ten genetic algorithm runs using the GOLDScore fitness function. The results of the docking studies presented in this work are the best binding results out of ten favorites predicted by Gold.

Supplementary material

CCDC 2093014 contains the supplementary crystallographic data for this paper. These data can be obtained free of charge from The Cambridge Crystallographic Data Centre *via* www.ccdc.cam.ac.uk/data_request/cif.

Acknowledgements

This study was supported financially by the Iran National Science Foundation (INSF). We would like to acknowledge the FAIRE (Frank H. Allen International Research and Education Programme) award of the Cambridge Structural Database, for suppling the access to the CSD softwares pakeage.

References

[1] R. Yendapally, R. E. Lee. *Bioorg. Med. Chem. Lett.* **2008**, *18,* 1607.
[2] H. X. Wei, D. Lu, V. Sun, J. Zhang, Y. Gu, P. Osenkowski, W. Ye, D. J. Selkoe, M. S. Wolfe, C. E. Augelli-Szafran. *Bioorg. Med. Chem. Lett.* **2016**, *26,* 2133.
[3] I. Declerck, B. Himpens, G. Droogmans, R. Casteels. *Pflügers Arch.* **1990**, *417,* 117.
[4] M. M. Weinberger. *Pediatr. Clin. N. Am.* **1975**, *22,* 121.
[5] S. J. Kwon, S. Y. Ko. *Tetrahedron Lett.* **2002**, *43,* 639.
[6] W. H. Frishman. *Circulation* **2003**, *107,* e117.
[7] D. T. Nash. *Clin. Cardiol.* **1990**, *13,* 764.
[8] Z. Mardani, R. Kazemshoar-Duzduzani, K. Moeini, A. Hajabbas-Farshchi, C. Carpenter-Warren, A. M. Z. Slawin, J. D. Woollins. *RSC Adv.* **2018**, *8,* 28810.
[9] Z. Mardani, M. Hakimi, K. Moeini, F. Mohr. *Acta Crystallogr.* **2019**, *C75,* 951.
[10] K. Chennakesava Rao, Y. Arun, K. Easwaramoorthi, C. Balachandran, T. Prakasam, T. Eswara Yuvaraj, P. T. Perumal. *Bioorg. Med. Chem. Lett.* **2014**, *24,* 3057.
[11] S. Vanguru, L. Jilla, Y. Sajja, R. Bantu, L. Nagarapu, J. B. Nanubolu, B. Bhaskar, N. Jain, S. Sivan, V. Manga. *Bioorg. Med. Chem. Lett.* **2017**, *27,* 792.
[12] M. Zhang, D.-M. Xian, H.-H. Li, J.-C. Zhang, Z.-L. You. *Aust. J. Chem.* **2012**, *65,* 343.
[13] M. D. Altıntop, A. Özdemir, G. Turan-Zitouni, S. Ilgın, Ö. Atlı, G. İşcan, Z. A. Kaplancıklı. *Eur. J. Med. Chem.* **2012**, *58,* 299.
[14] V. C. Da Silveira, J. S. Luz, C. C. Oliveira, I. Graziani, M. R. Ciriolo, A. M. D. C. Ferreira. *J. Inorg. Biochem.* **2008**, *102,* 1090.
[15] K. Shanker, R. Rohini, V. Ravinder, P. M. Reddy, Y.-P. Ho. *Spectrochim. Acta* **2009**, *A73,* 205.
[16] H.-W. Lin. *Synth. React. Inorg. Nano-Met. Chem.* **2009**, *39,* 73.
[17] M. Taha, N. H. Ismail, M. S. Baharudin, S. Lalani, S. Mehboob, K. M. Khan, S. Yousuf, S. Siddiqui, F. Rahim, M. I. Choudhary. *Med. Chem. Res.* **2015**, *24,* 1310.
[18] C. Jing, C. Wang, K. Yan, K. Zhao, G. Sheng, D. Qu, F. Niu, H. Zhu, Z. You. *Bioorg. Med. Chem.* **2016**, *24,* 270.
[19] J. R. Morrow, K. A. Kolasa. *Inorg. Chim. Acta* **1992**, *195,* 245.
[20] A. D. Tiwari, A. K. Mishra, S. B. Mishra, B. B. Mamba, B. Maji, S. Bhattacharya. *Spectrochim. Acta* **2011**, *A79,* 1050.
[21] E. M. Hodnett, W. J. Dunn. *J. Med. Chem.* **1970**, *13,* 768.
[22] E. M. Hodnett, W. J. Dunn. *J. Med. Chem.* **1972**, *15,* 339.
[23] V. R. Martínez, M. V. Aguirre, J. S. Todaro, O. E. Piro, G. A. Echeverría, E. G. Ferrer, P. a. M. Williams. *Toxicol. In Vitro* **2018**, *48,* 205.
[24] A. Adhikari, N. Kumari, M. Adhikari, N. Kumar, A. K. Tiwari, A. Shukla, A. K. Mishra, A. Datta. *Bioorg. Med. Chem.* **2017**, *25,* 3483.
[25] J. Dam, Z. Ismail, T. Kurebwa, N. Gangat, L. Harmse, H. M. Marques, A. Lemmerer, M. L. Bode, C. B. De Koning. *Eur. J. Med. Chem.* **2017**, *126,* 353.
[26] L. Saghatforoush, K. Moeini, S. A. Hosseini-Yazdi, Z. Mardani, A. Hajabbas-Farshchi, H. T. Jameson, S. G. Telfer, J. D. Woollins. *RSC Adv.* **2018**, *8,* 35625.
[27] F. Marandi, K. Moeini, F. Alizadeh, Z. Mardani, C. K. Quah, W.-S. Loh, J. D. Woollins. *Inorg. Chim. Acta* **2018**, *482,* 717−725.

[28] F. Marandi, K. Moeini, F. Alizadeh, Z. Mardani, C. K. Quah, W.-S. Loh. *Z. Naturforsch.* **2018**, *73b,* 369−375.
[29] F. Marandi, K. Moeini, A. Arkak, Z. Mardani, H. Krautscheid. *J. Coord. Chem.* **2018**, *71,* 3893−3911.
[30] Z. Mardani, V. Golsanamlou, Z. Jabbarzadeh, K. Moeini, S. Khodavandegar, C. Carpenter-Warren, A. M. Z. Slawin, J. D. Woollins. *J. Coord. Chem.* **2018**, *71,* 4109−4131.
[31] N. Shahabadi, L. Ghafari, Z. Mardani, F. Shiri. *Nucleos. Nucleot. Nucl.* **2021**, Accepted.
[32] M. Hakimi, Z. Mardani, K. Moeini. *J. Chem. Res.* **2013**, *37,* 140.
[33] M. Hakimi, Z. Mardani, K. Moeini, E. Schuh, F. Mohr. *Z. Naturforsch.* **2013**, *B68,* 272.
[34] M. Hakimi, Z. Mardani, K. Moeini, F. Mohr. *Polyhedron* **2015**, *102,* 569.
[35] F. H. Allen. *Acta Crystallogr.* **2002**, *B58,* 380–388.
[36] M. Hakimi, Z. Mardani, K. Moeini, F. Mohr, M. A. Fernandes. *Polyhedron* **2014**, *67,* 27–35.
[37] M. Hakimi, K. Moeini, Z. Mardani, F. Mohr. *Polyhedron* **2014**, *70,* 92.
[38] F. Marandi, K. Moeini, B. Mostafazadeh, H. Krautscheid. *Polyhedron* **2017**, *133,* 146−154.
[39] F. Marandi, K. Moeini, A. Arkak, Z. Mardani, H. Krautscheid. *J. Coord. Chem.* **2019**, *71,* 3893.
[40] Z. Mardani, V. Golsanamlou, S. Khodavandegar, K. Moeini, A. M. Z. Slawin, J. D. Woollins. *J. Coord. Chem.* **2018**, *71,* 120.
[41] G. Jones, P. Willett, R. C. Glen, A. R. Leach, R. Taylor. *J. Mol. Biol.* **1997**, *267,* 727−748.
[42] *https://www.drugs.com/mtm/doxorubicin.html*. 7/19/2018.
[43] A. Usman, H.-K. Fun, S. Chantrapromma, H.-L. Zhu, Q.-X. Liu. *Acta Crystallogr.* **2003**, *E59,* o215.
[44] J.-Y. Ma, B.-L. Lv, S.-H. Gu, J.-W. Guo, W.-P. Yin. *Acta Crystallogr.* **2006**, *E62,* m1322.
[45] T. Chattopadhyay, M. Mukherjee, K. S. Banu, A. Banerjee, E. Suresh, E. Zangrando, D. Das. *J. Coord. Chem.* **2009**, *62,* 967.
[46] S.-J. Peng, H.-Y. Hou, C.-S. Zhou. *Synth. React. Inorg. Nano-Met. Chem.* **2009**, *39,* 462.
[47] N. A. Ikmal Hisham, H. Khaledi, H. Mohd Ali. *Acta Crystallogr.* **2011**, *E67,* m932.
[48] Y. J. Wei, F. W. Wang, Q. Y. Zhu. *Acta Crystallogr.* **2008**, *E64,* m859.
[49] D. F. Zhang, M. H. Zhou, C. J. Yuan. *Acta Crystallogr.* **2008**, *E64,* m825.
[50] X.-Y. Qiu. *Acta Crystallogr.* **2006**, *E62,* m717.
[51] X.-F. Li, Z.-L. You, P. Hou, C.-L. Zhang. *J. Chem. Crystallogr.* **2010**, *40,* 561.
[52] S.-J. Peng, C.-S. Zhou, T. Yang. *Acta Crystallogr.* **2006**, *E62,* m1147.
[53] X. W. Zhu, X. Z. Yang. *Acta Crystallogr.* **2008**, *E64,* m1090.
[54] X. W. Zhu. *Acta Crystallogr.* **2008**, *E64,* m1456.
[55] S.-S. Qian, H.-H. Li, H. Zhu, Z.-M. Yang, Z.-L. You, H.-L. Zhu. *Synth. React. Inorg. Nano-Met. Chem.* **2013**, *43,* 412.
[56] Y. X. Sun, Z. L. You. *Synth. React. Inorg. Nano-Met. Chem.* **2007**, *36,* 359.
[57] F. Marandi, K. Moeini, H. Krautscheid. *Acta Crystallogr.* **2019**, *C75,* 1389.
[58] *STOE & Cie GmbH, X-Area Version 1.77, Darmstadt*. **2016**.
[59] G. Sheldrick. *Acta Crystallogr.* **2008**, *A64,* 112.
[60] L. J. Farrugia. *J. Appl. Crystallogr.* **1997**, *30,* 565–565.

[61] M. N. Burnett, C. K. Johnson, Ortep-III, Report ORNL-6895. Oak Ridge National Laboratory, Oak Ridge, Tennessee, U.S., **1996**.
[62] G. Bergerhof, M. Berndt, K. Brandenburg. *J. Res. Natl. Stand. Technol.* **1996**, *101,* 221–225.
[63] M. J. Frisch, G. W. Trucks, H. B. Schlegel, G. E. Scuseria, M. A. Robb, J. R. Cheeseman, G. Scalmani, V. Barone, B. Mennucci, G. A. Petersson, H. Nakatsuji, M. Caricato, X. Li, H. P. Hratchian, A. F. Izmaylov, J. Bloino, G. Zheng, J. L. Sonnenberg, M. Hada, M. Ehara, K. Toyota, R. Fukuda, J. Hasegawa, M. Ishida, T. Nakajima, Y. Honda, O. Kitao, H. Nakai, T. Vreven, J. A. Montgomery Jr., J. E. Peralta, F. Ogliaro, M. J. Bearpark, J. Heyd, E. N. Brothers, K. N. Kudin, V. N. Staroverov, R. Kobayashi, J. Normand, K. Raghavachari, A. P. Rendell, J. C. Burant, S. S. Iyengar, J. Tomasi, M. Cossi, N. Rega, N. J. Millam, M. Klene, J. E. Knox, J. B. Cross, V. Bakken, C. Adamo, J. Jaramillo, R. Gomperts, R. E. Stratmann, O. Yazyev, A. J. Austin, R. Cammi, C. Pomelli, J. W. Ochterski, R. L. Martin, K. Morokuma, V. G. Zakrzewski, G. A. Voth, P. Salvador, J. J. Dannenberg, S. Dapprich, A. D. Daniels, Ö. Farkas, J. B. Foresman, J. V. Ortiz, J. Cioslowski, D. J. Fox, *Gaussian 09*. **2009**, Gaussian, Inc.: Wallingford, CT, USA.
[64] J. P. Perdew. *Phys. Rev.* **1986**, *B33,* 8822.
[65] A. Gavezzotti. *Acc. Chem. Res.* **1994**, *27,* 309.

Table 1. The NBO analysis results for the ligand and complex **1**. The values are the average of charge on the similar atoms. The values of parentheses show the variation of charge on the atoms after coordination.

	C^{ar}	C^{imine}	$C^{aliphatic}$	H^{ar}	H^{imine}	$H^{aliphatic}$	H^{phenol}	$H^{alcohol}$	H^{amine}	N^{imine}	N^{amine}	O^{phenol}	$O^{alcohol}$	Br	Zn
Ligand	–0.11	0.12	–0.20	0.21	0.17	0.20	0.48	0.45	0.34	–0.5	–0.65	–0.65	–0.74	–	–
Complex **1**	–0.08 (0.03)	0.20 (0.08)	–0.13 (0.07)	0.17 (–0.04)	0.14 (–0.03)	0.21 (0.01)	–	0.43 (–0.02)	0.39 (0.05)	–0.65 (–0.15)	–0.48 (0.17)	–0.77 (–0.12)	–0.69 (0.05)	–0.61	0.94

Table 2. The calculated fitness values for complexes **1**–**3** and doxorubicin.

	B-DNA (maj)	B-DNA (min)	BRAF-Kinase	CatB	DNA-Gyrase	HDAC7	rHA	RNR	TrxR	TS	Top II
Ligand	41.35	55.98	39.76	45.46	48.79	51.69	42.24	41.56	36.60	42.55	45.05
Complex **1**	39.22	57.64	43.24	49.42	52.73	55.06	46.07	41.44	37.59	43.86	46.22
Complex **2**	40.49	58.80	43.92	51.17	51.72	52.72	45.10	42.69	34.82	43.33	46.82
Complex **3**	39.32	57.89	47.72	44.73	52.26	56.95	46.07	43.47	35.54	46.01	50.84
Doxorubicin	33.47	83.10	54.21	25.95	52.97	50.73	50.10	49.18	66.70	53.34	59.05

Table 3. Crystal structure data and structure refinement of complex **1**.

Empirical formula	$C_{11}H_{16}Br_2N_2O_2Zn$
Formula weight, g mol^{-1}	433.45
Crystal size, mm^3	0.15 × 0.09 × 0.09
Temperature, K	293
Crystal system	Triclinic
Space group	$P\bar{1}$
Unit cell dimensions (Å, °)	
a	7.4429(4)
b	8.8917(5)
c	11.4799(7)
α	90.676(5)
β	96.614(5)
γ	109.297(5)
Volume, Å^3	711.28(7)
Z	2
Calculated density, g cm^{-3}	2.510
Absorption coefficient, mm^{-1}	7.37
F(000), *e*	532
θ range data collection, °	2.4–28.0
h, *k*, *l* ranges	$-9 \le h \le 9$, $-11 \le k \le 11$, $-14 \le l \le 14$
Reflections collected / independent / R_{int}	22895 / 3112/ 0.043
Data / ref. parameters	3112 / 164
*R*1 / *wR*2 ($I > 2\,\sigma(I)$)	0.0799/0.02492
*R*1 / *wR*2 (all data)	0.0896 / 0.2524
Goodness-of-fit on F^2	1.18
Largest diff. peak / hole, *e* Å^{-3}	2.15 / −1.60

Table 4. Selected bond lengths (Å) and angles (°) for complex **1** with estimated standard deviations in parentheses[a].

Bond lengths		Angles	
Zn03−Br01	2.385(3)	Br02−Zn03−Br01	112.69(10)
Zn03−Br02	2.367(3)	O004−Zn03−Br01	111.0(4)
Zn03−O004	1.956(11)	O004−Zn03−Br02	109.7(4)
Zn03−N7	2.007(14)	O004−Zn03−N7	96.8(5)
		N7−Zn03−Br01	113.6(4)

Table 5. Hydrogen bond dimensions (Å and °) in complex **1**.

D–H···A	*d*(D–H)	*d*(H···A)	*d*(D···A)	<(DHA)	Symmetry code on A atom
C00c–H00e···Br02	0.93	2.981	3.79(2)	147	−1+*x*, −1+*y*, *z*
C00h–H00m···Br02	0.97	2.972	3.89(2)	160	1+*x*, *y*, *z*
N006–H00B···O004	0.89	1.91	2.76(2)	159	1+*x*, *y*, *z*
N006–H00A···O007	0.89	2.17	2.96(2)	147	2−*x*, 1−*y*, 1−*z*
C00b–H00c···Br02	0.97	3.049	3.69(2)	125	2−*x*, 2−*y*, 1−*z*
C00b–H00d···Br01	0.97	2.954	3.69(2)	133	1+*x*, *y*, *z*
C00f–H00i···Br01	0.97	3.032	3.83(2)	141	2−*x*, 1−*y*, 1−*z*
O007–H007···N006	0.82	2.47	2.96(2)	119	2−*x*, 1−*y*, 1−*z*
O007–H007···O007	0.82	2.77	3.24(2)	164	2−*x*, 1−*y*, 1−*z*

Figure Captions

Figure 1. Structure of the 2-(((2-((2-hydroxyethyl)amino)ethyl)imino)methyl)phenol ligand (L).

Figure 2. Ortep-III diagram of the molecular structure of complex **1**. The ellipsoids are drawn at the 50% probability level.

Figure 3. Packing of molecules **1**, showing the $R_6^6(44)$ motif. Each $ZnNOBr_2$ unit is shown as tetrahedral (light blue). Only hydrogen atoms participate in hydrogen bonding are shown.

Figure 4. All coordination modes of the 2-(((2-((2-hydroxyethyl)amino)ethyl)imino)methyl)phenol ligand (L) among the CSD.

Figure 5. Structure of unit searched for CSD analogues of complex **1**. X refers to the any halogen atom.

Figure 6. Docking study result, showing the interaction between ligand and B-DNA. a) docking into major groove, b) docking into minor groove.

Figure 7. Docking study result, showing the interaction between complex **1** and B-DNA. a) docking into major groove, b) docking into minor groove

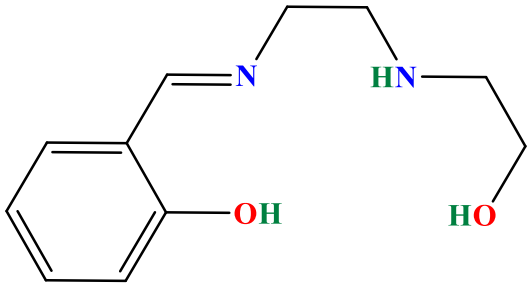

Figure 1.

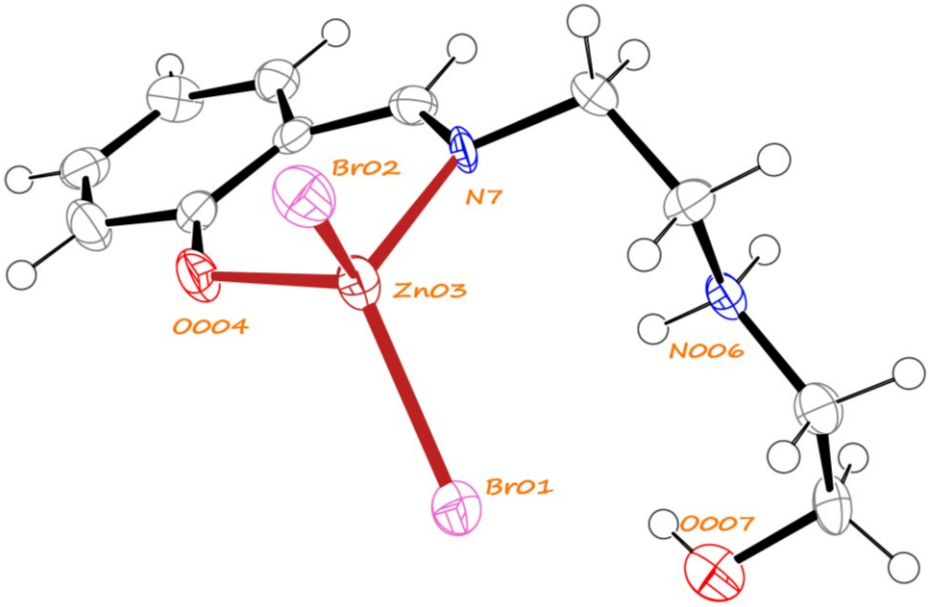

Figure 2.

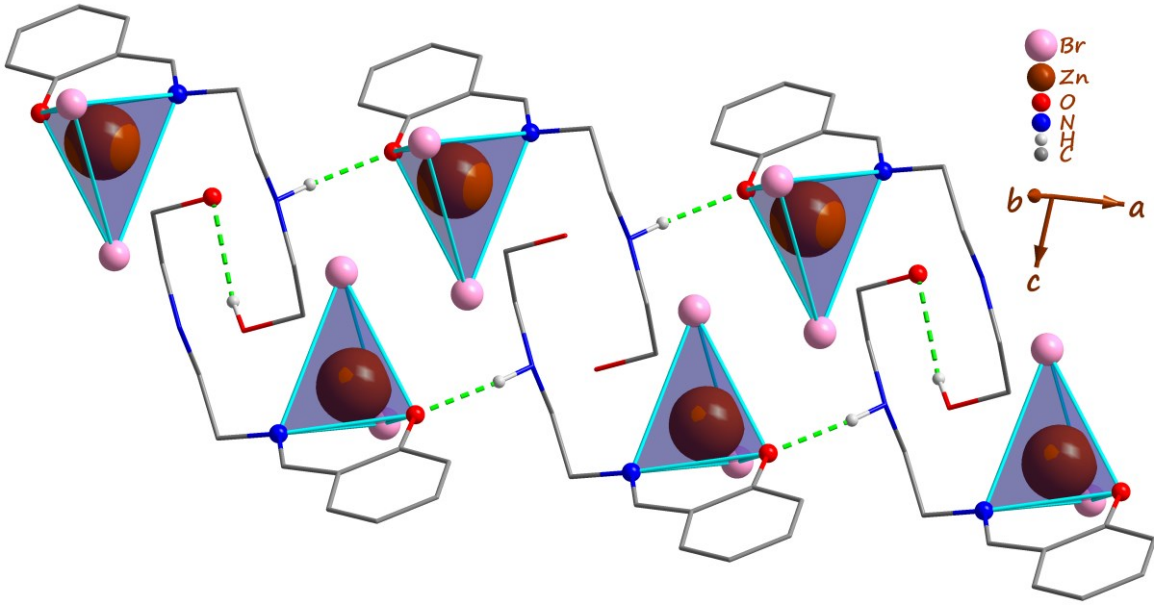

Figure 3.

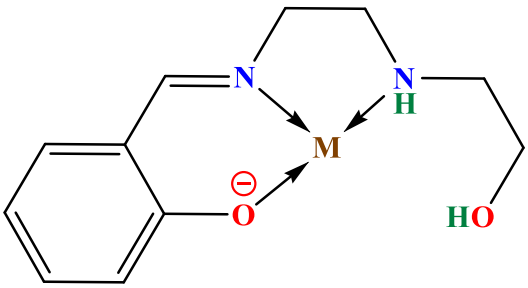

($O^{phenol}N^{imine}N^{amine}$)

63%

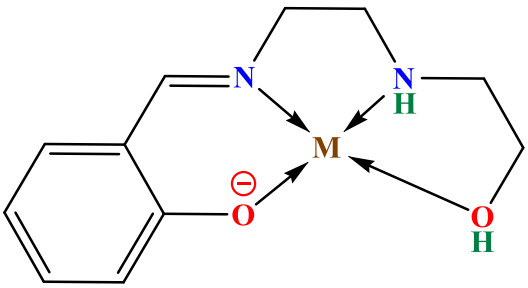

($O^{phenol}N^{imine}N^{amine}O^{alcohol}$)

25%

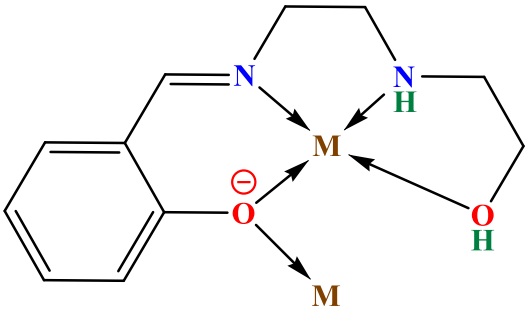

(μ–$O^{phenol}N^{imine}N^{amine}O^{alcohol}$)

9%

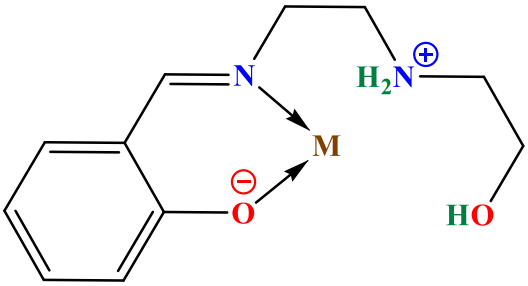

($O^{phenol}N^{imine}$)^z

3%

Figure 4.

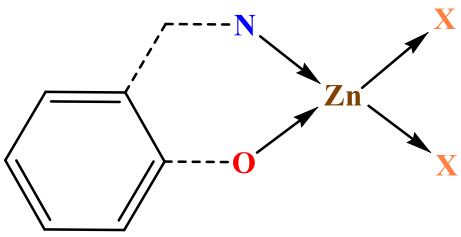

Figure 5.

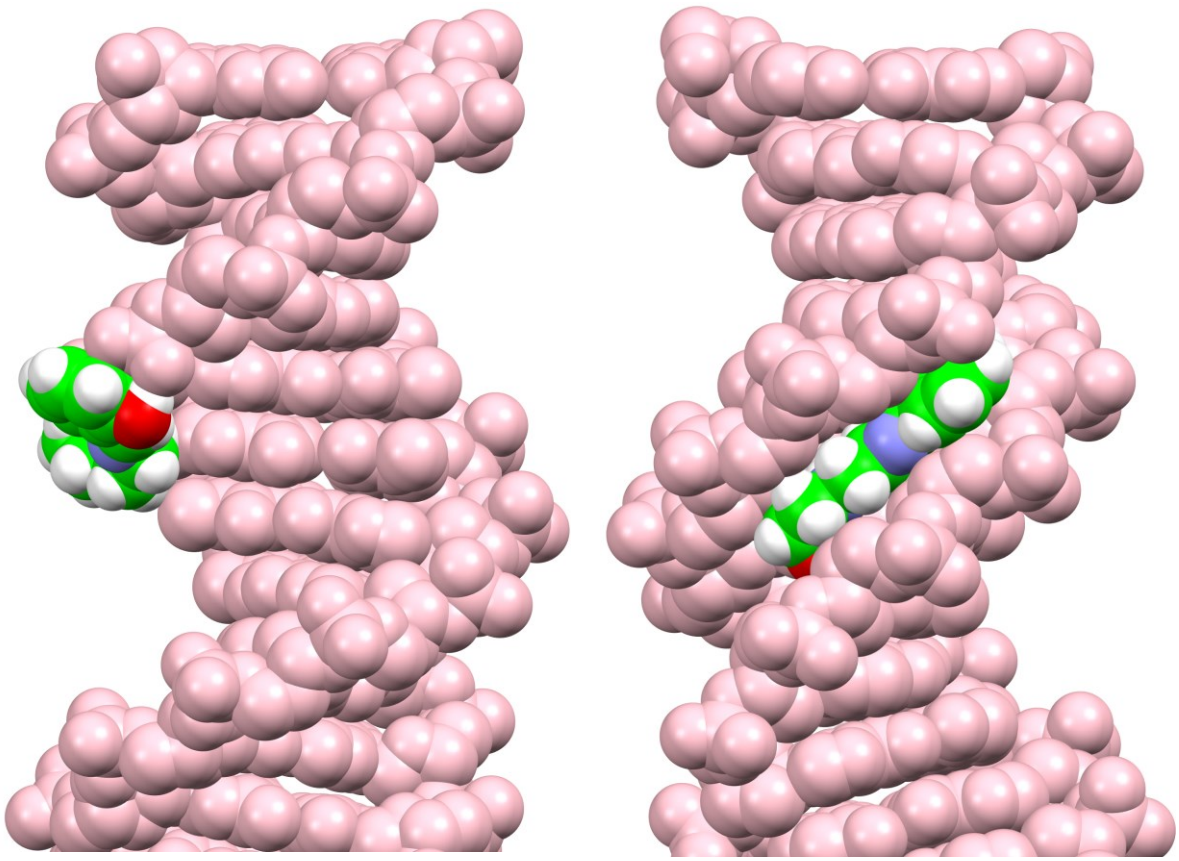

a b

Figure 6.

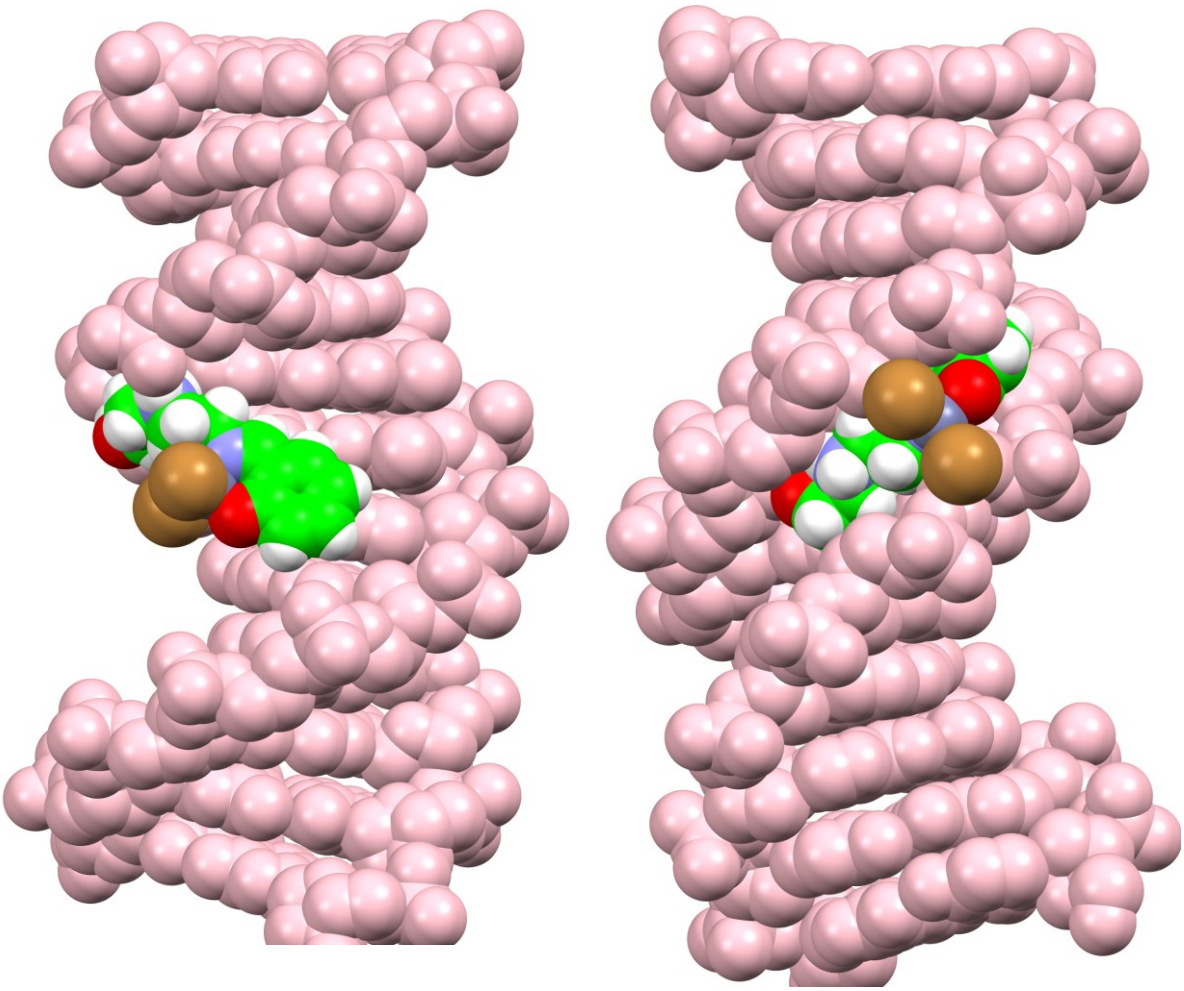

a b

Figure 7.